

# Sports Video Object Tracking Algorithm Based on Optimized Particle Filter

Qingbao Wang<sup>1</sup>, Chenbo Zhao<sup>2,\*</sup>

<sup>1</sup> College of Physical Education, Baicheng Normal University, Baicheng, Jilin 137000, China

<sup>2</sup> School of Physical Education, Jiamusi University, Jiamusi, Heilongjiang 154007, China

## Abstract

**INTRODUCTION:** With the continuous development of video analysis technology, sports video object tracking has become one of the research hotspots. Particle filter, as an effective object tracking algorithm, has been widely used in sports video object tracking. However, traditional particle filters have some shortcomings, such as particle depletion and high computational complexity, which require optimization. This article proposes a sports video object tracking algorithm based on optimized particle filters, aiming to improve the accuracy and stability of object tracking. Particle filter-based human motion video target tracking technology has become a trend. This project intends to apply particle filters to image processing of human activities. Firstly, an improved particle filter model tracks moving video objects. The purpose is to improve the tracking effect further and increase the accuracy. HSV distribution model was used to establish a target observation model. The algorithm is combined with the weight reduction algorithm to realize the human motion trajectory detection in the target observation mode. An examination of sports player videos then confirmed the model. Experiments show that this method can be used to track people in moving images of sports. Compared with other methods, this method has higher computational accuracy and speed.

**Keywords:** Moving target detection, Gaussian mixture model, Particle filter, RGB colour columnar structure

Received on 22 September 2023, accepted on 20 October 2023, published on 23 October 2023

Copyright © 2023 Q. Wang *et al.*, licensed to EAI. This is an open access article distributed under the terms of the [CC BY-NC-SA 4.0](https://creativecommons.org/licenses/by-nc-sa/4.0/), which permits copying, redistributing, remixing, transformation, and building upon the material in any medium so long as the original work is properly cited.

doi: 10.4108/eetsis.3935

\*Corresponding author. Email: zhaochenbo@jmsu.edu.cn

## 1. Introduction

Target tracking technology was initially used on a military scale and then quickly spread to the civilian population. The target tracking technique is to observe the characteristics and states of the tracked objects to obtain their changes at various time points. This change is analyzed, and the target tracking is achieved. A series of images must be processed to detect moving objects. It is mainly to extract, identify, track the target, and obtain the tracked object's acceleration, speed, position and other information. Accurate tracking of moving objects in complex environments has become the focus of scientific workers. Among these methods, the inter-frame difference method has the advantages of less computation and better real-time performance. However, if a relatively uniform

relationship exists between the background and the measured object in the image, the recognition effect will become poor. The background subtraction method can obtain a more comprehensive image of the object. The system is suitable for high-reliability security monitoring work. However, this method has disadvantages such as low real-time performance and long operation time. An improved particle filters DE multi-target detection and tracking algorithm is proposed in reference [1]. An image processing method based on dynamic Gaussian distribution features is proposed. The method is combined with the weighted particle filter to recognize the object of interest. In reference [2], an improved particle filter preprocessing method was studied to preprocess small and large targets under complex conditions. Then, a particle filtering method based on Weibull clutter is proposed. It is very resistant to loud noises. The Gaussian mixture method has apparent advantages in suppressing

interference such as occlusion and illumination. Using RGB color column structure can better prevent color drift and artificial interference.

Particle filters based on the Monte Carlo method play an important role in nonlinear and non-Gaussian problems. This method can be used well in object tracking. Reference [3] proposes an object-tracking algorithm based on a particle filter with mean transform. Reference [4] proposes an improved particle filter target tracking method based on adaptive fusion of color characteristics. Literature [5] uses Laplace's algorithm to solve this problem. This paper presents an algorithm based on hybrid optimization. An improved particle filter algorithm and the Gaussian filter algorithm are proposed. This algorithm improves the shortcomings of the traditional particle filter model. Survival of the fittest and group evolution are its core ideas. The algorithm has high optimization performance in the initial stage and fast convergence in the initial stage. This algorithm can effectively solve the problem of particle degradation. Then, the particle filtering method of the Gaussian filter is proposed to improve the difference between particles. In this way, deterioration of the particles can be avoided. At the same time, the target observation model is established by using the spatial distribution model of HSV. Then, the algorithm is combined with the weight reduction algorithm to realize the detection of human motion images in the target observation mode [6]. Specific trials used video recordings of athletes. Experiments show that this method can track moving objects well without relying on existing data. The results show that the method is feasible and effective.

The application of particle filters in sports video object tracking can address the unique challenges of sports video tracking by customizing optimization strategies through the following methods.

In sports videos, prior knowledge can be fully utilized to optimize the performance of particle filters, such as athletes' motion patterns and ball trajectories. This can be achieved by introducing this prior knowledge into the filter or considering these factors when calculating particle weights. In sports videos, the motion mode and speed of the target object may undergo significant changes, which requires particle filters to be able to adaptively adjust their parameters. For example, the sampling frequency of particles can be adjusted based on the motion speed of the target object, or the weight allocation of particles can be adjusted based on the shape changes of the target object. In sports videos, the target object may be obstructed or deformed by other objects, which can pose challenges to tracking. To address this issue, it is possible to introduce object occlusion and deformation detection algorithms into particle filters or consider the effects of occlusion and deformation when calculating weights.

These methods are all aimed at customizing optimization strategies to address the unique challenges of sports video tracking. The optimization of these strategies will help improve the performance and computational

ability of particle filters in sports video object tracking, thereby providing more accurate and reliable tools and methods for sports video analysis.

## 2. Introduction of particle filter

The state vector  $f$  of the particle filter is defined.

$$f = [i_a, i_b, v_{i_a}, v_{i_b}] \quad (1)$$

$i_a$  represents the transverse coordinates of the sample image center and  $i_b$  represents the longitudinal coordinates of the sample image center.  $v_{i_a}$  represents the speed at the  $i_a$  coordinate and  $v_{i_b}$  represents the speed at the  $i_b$  coordinate. The center of estimation of the moving object can be obtained from equation (2):

$$W = \sum_{i=1}^l \lambda_i \cdot f_t^i \quad (2)$$

$f_t^i$  is particle  $i$  at time  $t$ .  $\lambda_i$  represents the mass of the particle  $i$ .  $l$  is the number of particles. A set of samples was identified as follows:

$$f_t = C f_{t-1} + \sigma_{t-1} \quad (3)$$

$$C = \begin{bmatrix} 1 & 0 & 1 & 0 \\ 1 & 0 & 1 & 0 \\ 0 & 1 & 0 & 1 \\ 0 & 0 & 1 & 0 \\ 0 & 0 & 0 & 1 \end{bmatrix} \quad (4)$$

$f_t$  represents the position of the particle at time  $t$ .

$C$  represents an essential element in the pattern.  $\sigma_{t-1}$  is Gaussian random white noise.

## 3. Improve the tracking method of particle filter

### 3.1 Dynamic background modelling based on the Gaussian mixture model

Once a foreground object is found, it can be tracked and analysed accordingly. Therefore, object detection is an essential link in object tracking [7]. Factors such as local occlusion and illumination greatly influence object detection accuracy. In the target tracking process, the Gaussian mixture model is applied to the background analysis of the target image. In this way, a dynamic background of a moving object can be obtained. An expression to determine the Gaussian mixture mode is given in equation (5). The process of Gaussian mixture

modelling is shown in Figure 1.

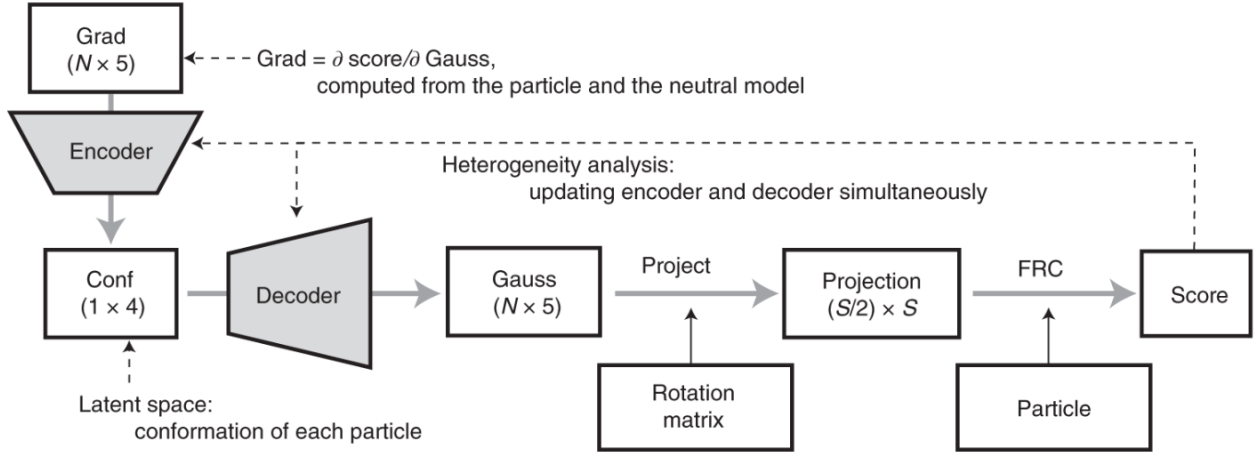


**Figure 1.** Establishment process of Gaussian mixture model

$$g(i_a) = \sum_{t=1}^T \rho_t O(i_a | \alpha_t) \quad (5)$$

$O(i_a | \alpha_t), t=1, 2, \dots, T$  represents the probability distribution of cluster  $t$ . Where  $\alpha_t$  is the corresponding vector.  $\rho_t$  represents the weighting factor of  $t$  in the cluster.  $0 \leq \rho_t \leq 1$  and  $\sum_{t=1}^T \rho_t = 1, T$  are the sum of the parts in the finite hybrid mode.

Assuming  $O(i_a | \alpha_t)$  is Gaussian, then  $g(i_a)$  is a mixed Gaussian distribution [8]. Where  $i_{a_i}$  represents  $i$  pixel point in the image,  $i=1, 2, \dots, l$ . The current probability distribution of pixels is a linear  $T$  order combination.  $\Lambda_j$  is the first category of  $j$ ,  $j=1, 2, \dots, T$ . The probability distribution function for  $i_{a_i}$  is shown as follows:

$$o(i_{a_i}) = \sum_{j=1}^T \rho_{ij} o(i_{a_i} | \Lambda_j) \quad (6)$$

In Gaussian distribution  $\rho_{ij}$ ,  $o(i_{a_i} | \Lambda_j)$  represents the scale coefficient [9]. It meets the requirements of  $0 \leq \rho_{ij} \leq 1$  and  $\sum_{t=1}^T \rho_{ij} = 1$ . Each Gaussian distribution  $o(i_{a_i} | \Lambda_j)$  is expressed in the Gaussian mixture model as:

$$o(i_{a_i} | \Lambda_j) = \frac{1}{\sqrt{2\rho\sigma_j^2}} \exp\left(-\frac{(i_{a_i} - \mu_j)^2}{2\sigma_j^2}\right) \quad (7)$$

$\mu_j$  stands for the mean of the Gaussian distribution.  $\sigma_j$

represents the covariance of the Gaussian distribution. The logarithmic likelihood function can be obtained from formula (2):

$$H(\alpha) = \sum_{i=1}^l \ln \left( \sum_{j=1}^T \rho_{ij} o(i_{a_i} | \Lambda_j) \right) \quad (8)$$

The posterior probability of the  $i$  pixel can be expressed as:

$$o(\Lambda_j | i_{a_i}) = \frac{\rho_{ij} o(i_{a_i} | \Lambda_j)}{\sum_{t=1}^T \rho_{it} o(i_{a_i} | \Lambda_t)} \quad (9)$$

Logarithmic likelihood functions are often implemented using empirical solutions:

$$W(\alpha) = -H(\alpha) = -\sum_{i=1}^l \ln \left( \sum_{j=1}^T \rho_{ij} o(i_{a_i} | \Lambda_j) \right) \quad (10)$$

Equation (10) requires minimal processing to obtain a maximum logarithmic likelihood. In other words:

$$\gamma(\alpha^{old} | \alpha^{new}) = -\sum_{i=1}^l \sum_{j=1}^T o^{old}(i_{a_i} | \Lambda_j) \cdot \ln(\rho_{ij} o^{new}(i_{a_i} | \Lambda_j)) \quad (11)$$

$\gamma$  represents a function of error. To obtain  $\gamma$  maximum logarithmic likelihood,  $A$  needs to be minimized. And replace the optimal parameter in formula (9).

### 3.2 Iterative, recursive particle filter based on RGB colour columnar structure

A modified particle filter is used to preprocess moving objects. The use of RGB colour column structure minimizes colour drift and artificial interference. In Figure 2, we can see an iterative, recursive particle filtration process [10]. This paper estimates the maximum value of the three colours. The following formula estimates the brightness value of each pixel:

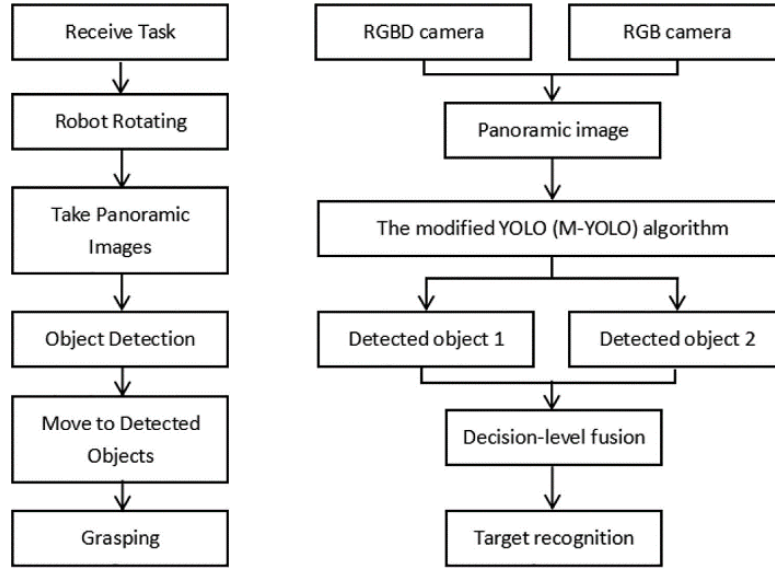


**Figure 2.** Flow chart of particle filtration based on colour bar graph iteration and recurrence

$$H(i_a, i_b) = \max(R_R(i_a, i_b), R_G(i_a, i_b), R_B(i_a, i_b)) \quad (12)$$

$R$  refers to the input screen.  $G$  stands for "Green channel".  $B$  stands for Blue Channel [11]. The iterative recurrence filter accomplishes the two-dimensional filter for preserving edges ( $\Theta$ ). Set the number of duplicates to 3. The primary layer is defined based on the filter estimates:

$$Y(i_a, i_b) = \Theta(H(i_a, i_b)) \quad (13)$$

$H$  indicates a brighter picture. The fairing factor is set at 0.3. The output image  $R$  is represented in the following form:

$$R(i_a, i_b) = Y(i_a, i_b) \cdot C(i_a, i_b) \quad (14)$$

After the iterative recursive estimation of the bottom layer  $Y$ , the bottom layer  $C$  is extracted RGB components. Here's how:

$$C_R(i_a, i_b) = R_R(i_a, i_b) / Y(i_a, i_b) \quad (15)$$

$$C_G(i_a, i_b) = R_G(i_a, i_b) / Y(i_a, i_b) \quad (16)$$

$$C_Y(i_a, i_b) = R_Y(i_a, i_b) / Y(i_a, i_b) \quad (17)$$

Then the weighting of particle  $i$  can be expressed as:

$$\lambda_i = \frac{1}{\sqrt{2\rho\sigma_j}} e^{-\frac{(1-\rho[o_f, q])}{2\sigma_j^2}} \quad (18)$$

$q$  refers to the color distribution of the tracked object.

$o_f$  represents the distribution of the extracted states.

### 3.3 Moving target detection based on global optical flow diagram

The Horn-Schunk method calculates the optical flow field

simply and conveniently, thus obtaining the optical flow direction quantity diagram [12]. The optical flow field becomes more significant at the moving position. According to the relationship between the optical flow field and the sports field, we can set a threshold and threshold the obtained optical flow diagram to obtain a general moving area. After a series of basic image processing, an accurate moving area detection graph is obtained. By processing the image frames in the video, moving objects can be accurately tracked in the static background [13]. The time domain change rate of the point on the dynamic image is the time domain change rate of the point on the dynamic image. When solving the optical flow equation, additional restrictions must be added, and according to the added restrictions, they are divided into various types. This paper will use the Horn-Schunck method to calculate the entire optical flow. Enter each of the three images into the sequence. The global optical flow pattern is a vector pattern through the global optical flow analysis. The global optical flow map uses thresholding, smoothing and morphological algorithms to locate moving targets. The positioning information of the moving objects in each picture can be obtained by processing all the same video images, and then the moving objects can be detected and tracked in the static environment [14]. Based on analysing the existing data, the data is filtered effectively. Therefore, the open and close operation of the image is used to filter it, and the discrete points belonging to the same moving object form a connected domain to obtain a more accurate detection of the moving object. Finally, the number of moving objects detected and the location value are obtained by connecting the blocks and combining them with the original image. The whole system is programmed in MATLAB so that the whole system can calculate the



global optical flow. The experimental image used here is the competitive image captured by the camera without moving, and the first three frames of images are processed

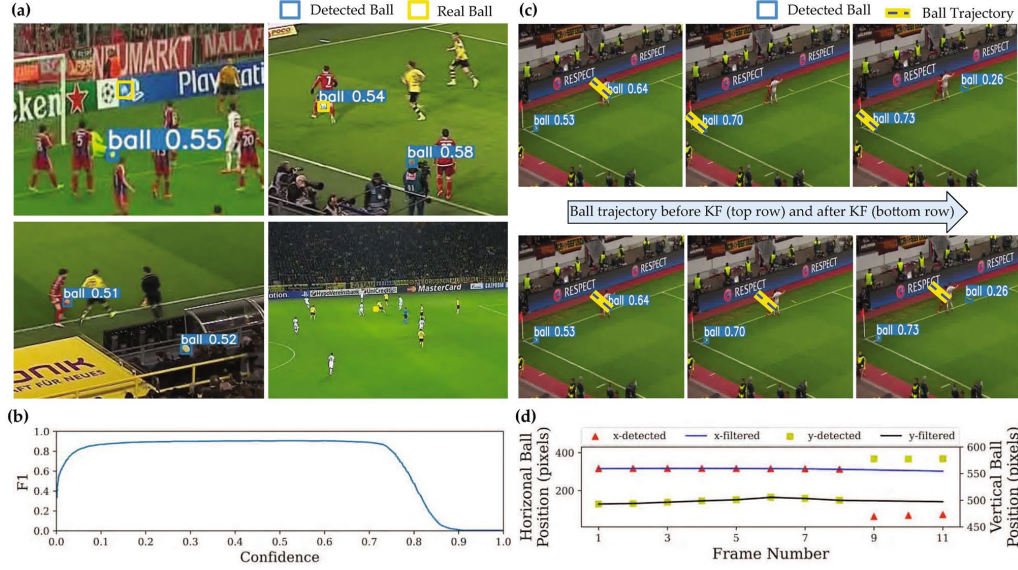


Figure 3. Sports images

## 4. Analysis and verification of simulation results

### 4.1 Numerical simulation

A classical and commonly used robust nonlinear non-Gaussian model is used as the simulation object. The process model is shown as follows:

$$X_k = 1 + \sin(0.04\pi k) + 0.5X_{k-1} + W_k \quad (19)$$

The measurement model is shown as follows

$$Z_k = \begin{cases} 0.2X_k^2 + V_k & k \leq 30 \\ 0.5X_k - 2 + V_k & k > 30 \end{cases} \quad (20)$$

Where the process noise is represented as  $w_k \Gamma(3, 2)$ , the observed noise is denoted by  $v_k N(0, 1E-5)$ . The simulation time is set to 60s.

Figure 4 shows data from a separate experiment. The figure shows that the particle filter has the best applicability in the Gaussian nonlinear mode [15]. It is close to the actual situation. There are deviations from the actual data in particle filters and in extended Kalman algorithms. A total of 100 autonomous experiments were done in this paper. The advantages and disadvantages of extended Kalman and odorless particle filters are quantified and compared. The three methods are compared, and their mean deviation curves are obtained. The results show that the tasteless particle filter is much better than the general Kalman and particle filters. Table 1

(Figure 3 is quoted in Automated soccer head impact exposure tracking using video and deep learning):

lists the three algorithms' time, mean square error and variance in 100 simulation tests. The results show that the Kalman particle filter is much better than the generalized particle filter in terms of mean and variance of mean square error, but its computational complexity is higher.

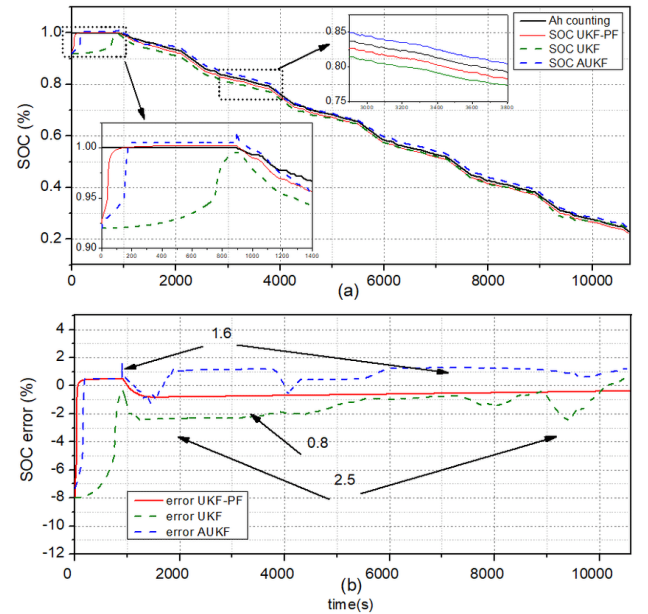


Figure 4. Estimated results of particle filter, extended Kalman and doorless particle filter

**Table 1.** Comparison of filtering performance of particle filter, extended Kalman and doorless particle filter

Algorithm	Root means square error mean	Root means square error variance
Particle filter	0.4177	0.0695
Extended Kalman particle filter	0.3369	0.0205
Odourless particle filter	0.0746	0.0095

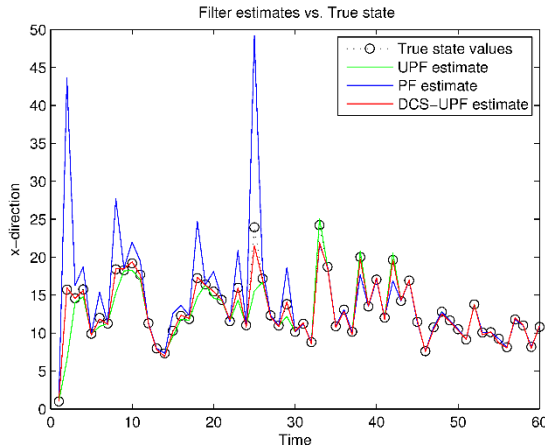
## 4.2 Video tracking simulation

An image containing 391 frames was simulated. In this paper, three filtering methods are compared and analyzed. The dimensions of this film are 384x288. The relevant calculation methods are implemented in a PC with 1 G and 43.0 GHz memory. This method is accomplished by using a hybrid program of VC++ and Matlab2011a. The standard particle filter has better tracking results [16]. A standard color-based filter diverges in about 320 frames. In this way, the target object is lost to tracking. Articles 2 and 3 of Figure 5 are the results of simulations of generalized Kalman and odorless particle filters. However, the generalized Kalman algorithm has some defects, such as solid volatility and poor stability, and its stability is not as good as the effect of odorless particle filter tracking.

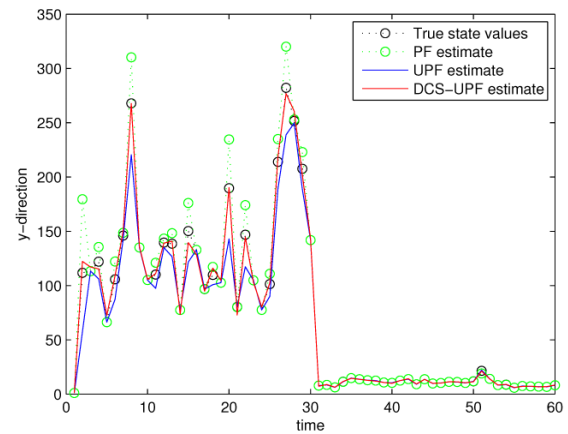
We will choose a key framework from the 10 frameworks. The goal is to compare the various tracking methods. Figure 6 compares tracking errors in the X and Y directions of the tracking position and the reference position in the three different methods. The baseline position is the target's actual location, which needs to be manually determined [17]. The results show that the odourless particle filter is superior to the extended Kalman particle filter in tracking. Tracking with ordinary particle filters is the least accurate. Evans et al. [18] proposed a new feature called distance intensity to extract changes in intensity from underwater sequences in local neighborhoods using the WH kernel. The possibility of these feature intensities is integrated into the particle filter framework to track objects of interest in underwater sequences. Panda and Nanda [19] proposed a particle filter based algorithm for tracking moving objects in complex real-world environments with shadows, dynamic entities in the background, adverse weather conditions, and lighting changes. Specifically, we attempt to establish an effective target and scene model by adhering to the concept of feature fusion.

The real-time performance of this method is related to computer configuration, particle number, particle filtering method and other factors. Table 2 shows the average tracking rate of fps per second (frame) for the three methods. The experimental results show that these methods meet the requirements of target tracking simulation well. The practical implementation depends on the particular chip and hardware environment used.

**Figure 5.** Tracking effect comparison



(a) x direction tracking error



(b) y direction tracking error

**Figure 6.** Comparison of tracking errors**Table 2.** Calculation cost comparison of the three algorithms

Video	Particle filter (fps)	Expansion Kalman (fps)	Odourless particle filter (fps)
Experimental sequence	24.4	15.3	10.9

## 5. Conclusion

This article analyzes an improved particle filter model for tracking sports transportation video objects. Firstly, a mathematical model for ground target observation was established using the HSV distribution model. This algorithm combines Gaussian filters to detect athlete images and videos in target observation mode. The specific experiment used athlete videos. This article quantifies and compares the advantages and disadvantages of ordinary particle filters, extended Kalman filters, and odorless particle filters. A comparison was made between these three methods. The results indicate that the generalized Kalman algorithm has some shortcomings, such as poor solid volatility and stability, and its stability is not as good as the tracking effect of odorless particle filters. The odorless particle filter is much better than ordinary Kalman filters and particle filters. Using regular particle filters for tracking is the least accurate. Experiments have shown that this method can effectively track moving targets without prior knowledge. The experimental results demonstrate the effectiveness and superiority of this method.

However, this method heavily relies on estimating the initial state. If the initial state estimation is not accurate, the filter may converge quickly or diverge quickly. There is also a problem of particle degradation. Because sampling based on weight can result in a shortage of particles when the weight is low, resulting in the loss of some data. In the future, an adaptive resampling strategy can be adopted, which dynamically adjusts the sampling

frequency based on the weight of particles, making the probability of particles with higher weights being sampled higher. In addition, mutation strategies such as random mutation or adaptive mutation can also be introduced to increase particle diversity and prevent particle depletion.

## Funding

This work was supported by Sports Science Research Project of Jilin Provincial Sports Bureau in 2023: Research on the implementation strategy of "ice and snow into campus" in Jilin University in post-Winter Olympics era (No:202352).

## References

- [1] Liu, Y., & Ji, Y. Target recognition of sport athletes based on deep learning and convolutional neural network. *Journal of Intelligent & Fuzzy Systems*, 2021;40(2): 2253-2263.
- [2] Abdelbaky, A., & Aly, S. Two-stream spatiotemporal feature fusion for human action recognition. *The Visual Computer*, 2021; 37(7): 1821-1835.
- [3] Liu, N., & Liu, P. Goaling recognition based on intelligent analysis of real-time basketball image of Internet of Things. *The Journal of Supercomputing*, 2022; 78(1): 123-143.
- [4] Cai, H. Application of intelligent real-time image processing in fitness motion detection under internet of things. *The Journal of Supercomputing*, 2022; 78(6): 7788-7804.
- [5] Zhang, X. Application of human motion recognition utilizing deep learning and smart wearable device in sports. *International Journal of System Assurance Engineering and Management*, 2021;12(4): 835-843.

- [6] Hao, Z., Wang, X., & Zheng, S. Recognition of basketball players' action detection based on visual image and Harris corner extraction algorithm. *Journal of Intelligent & Fuzzy Systems*, 2021; 40(4): 7589-7599.
- [7] Liu, A., Xie, H., & Ahmed, K. Fault detection technology of national traditional sports equipment based on optical microscope imaging technology. *Alexandria Engineering Journal*, 2021; 60(2): 2697-2705.
- [8] Şah, M., & Direkçöglü, C. Review and evaluation of player detection methods in field sports: Comparing conventional and deep learning based methods. *Multimedia Tools and Applications*, 2023; 82(9): 13141-13165.
- [9] Papic, C., Sanders, R. H., Naemi, R., Elipot, M., & Andersen, J. Improving data acquisition speed and accuracy in sport using neural networks. *Journal of Sports Sciences*, 2021; 39(5): 513-522.
- [10] Tsai, M. F., & Huang, S. H. Enhancing accuracy of human action Recognition System using Skeleton Point correction method. *Multimedia Tools and Applications*, 2022; 81(5): 7439-7459.
- [11] Abdelbaky, A., & Aly, S. Human action recognition using three orthogonal planes with unsupervised deep convolutional neural network. *Multimedia Tools and Applications*, 2021; 80(13): 20019-20043.
- [12] Gao, H., Xu, K., Cao, M., Xiao, J., Xu, Q., & Yin, Y. The deep features and attention mechanism-based method to dish healthcare under social IoT systems: an empirical study with a hand-deep local-global net. *IEEE Transactions on Computational Social Systems*, 2021; 9(1): 336-347.
- [13] Hao, L., & Pandey, H. M. Research on the Positioning Technology of Sports 3D Teaching Action Based on Machine Vision. *Mobile Networks and Applications*, 2022; 27(6): 2419-2428.
- [14] Li, J., & Gu, D. Research on basketball players' action recognition based on interactive system and machine learning. *Journal of Intelligent & Fuzzy Systems*, 2021; 40(2): 2029-2039.
- [15] Meng, L., & Qiao, E. Analysis and design of dual-feature fusion neural network for sports injury estimation model. *Neural Computing and Applications*, 2023; 35(20): 14627-14639.
- [16] Saqib, S., Ditta, A., Khan, M. A., Kazmi, S. A. R., & Alquhayz, H. Intelligent dynamic gesture recognition using CNN empowered by edit distance. *Cmc-Computers Materials & Continua*, 2021; 66(2): 2061-2076.
- [17] Cai, W., Wei, Z., Liu, R., Zhuang, Y., Wang, Y., & Ning, X. Remote sensing image recognition based on multi-attention residual fusion networks. *ASP Transactions on Pattern Recognition and Intelligent Systems*, 2021; 1(1): 1-8.
- [18] Evans L, Rhodes A, Alhazzani W, et al. Surviving sepsis campaign: international guidelines for management of sepsis and septic shock 2021. *Critical care medicine*, 2021, 49(11): e1063-e1143.
- [19] Panda J, Nanda P K. Particle filter-based video object tracking using feature fusion in template partition. *The Visual Computer*, 2023, 39(7): 2757-2779.